An overview of engineering numerical methods for the dynamic analysis of a nuclear reactor with fluid-structure interaction modelling

Jean-François Sigrist
DCNS Propulsion, Service Technique et Scientifique,
44620 La Montagne, France
E-mail: jean-francois.sigrist@dcnsgroup.com

ABSTRACT

The paper is concerned with the dynamic analysis of a nuclear reactor with fluid-structure interaction modelling. Various fluid-structure interaction effects (inertial, elasto-acoustic coupling, confinement) are investigated using specific mathematical modelling. In particular, modelling of the reactor internal structures is performed using an homogenisation method whose numerical basis are exposed in the paper. Influence of fluid-structure coupling on the dynamic behaviour of the reactor is highlighted with a modal analysis, on the one hand, and a dynamic analysis in the 0–20 Hz and 20–200 Hz frequency range, on the other hand. Modal analysis is carried out by computing the mode shapes, frequencies and effective masses of the reactor with and without fluid-structure interaction. Dynamic analysis is performed using various engineering methods (temporal and spectral approaches) which are compared and discussed. From the engineering standpoint, the following questions, of paramount interest in pre-design analysis, are addressed: i) What are the predominant coupling effects in the low frequency range (0–20 Hz)? ii) What are the predominant coupling effects in the high frequency range (20–200 Hz)? iii) What is the influence of the presence of internal structures as far as fluid-structure interaction is concerned? iv) What is the influence of the static pressure loading on the dynamic behaviour of the nuclear reactor?

Keywords: Finite element analysis, fluid-structure interaction, homogenisation method, dynamic analysis.

1. INTRODUCTION

The numerical simulation of fluid-structure interaction problems has made tremendous progress over the past decades: many numerical methods have been proposed to take these phenomena into account in various engineering domains, among which power nuclear engineering in seismic analysis [1,2,3]. Although such methods have been firmly validated from the theoretical, numerical and even experimental points of view [4,5,6] they are still scarcely used in the industrial domain in pre-design analysis.

As this is true in particular as far as naval propulsion is concerned, French naval shipbuilder DCNS has launched a R&D program in order to improve the engineering practices for the design of nuclear propulsion reactors. This generic study aims at analysing the relative importance of fluid-structure interaction mechanisms on the dynamic response of

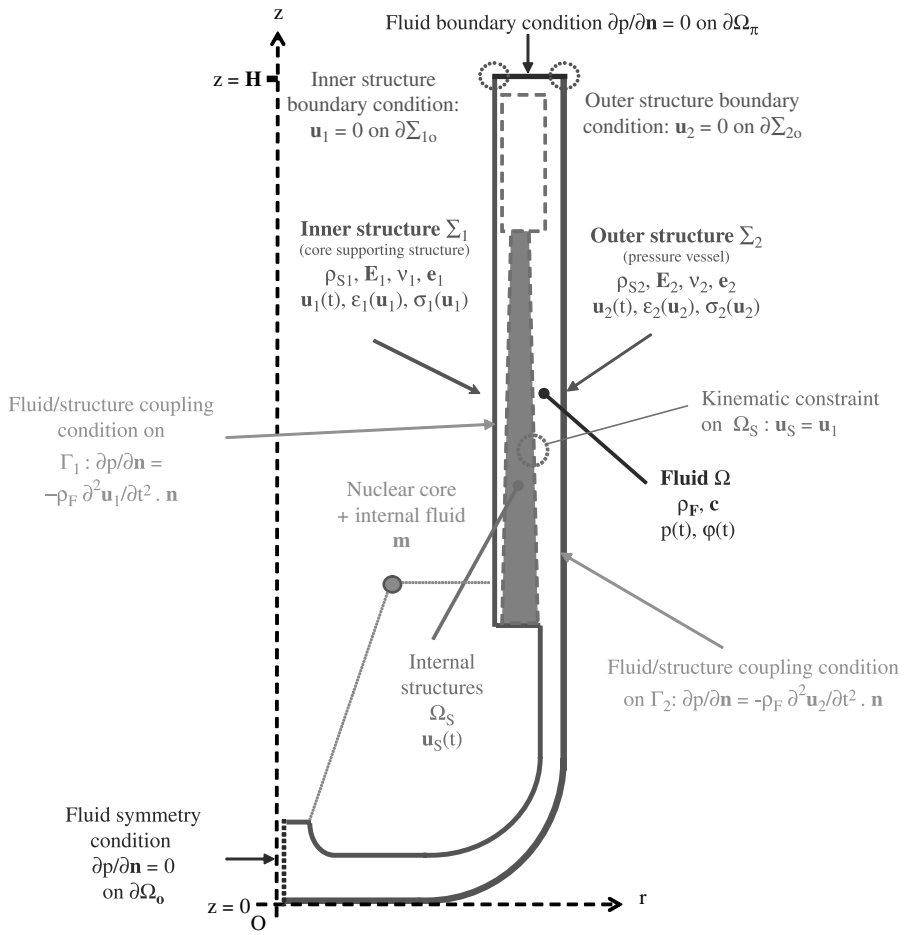

Figure 1 Simplified model of the nuclear reactor: outer structure (pressure vessel), inner structure (core support) and internal structures.

a nuclear propulsion reactor when subjected to seismic or shock excitation. Seismic analysis is of major concern as far as ground prototype reactors are concerned, while shock analysis is of paramount importance for embarked reactors. In the latter case, "shock analysis" refers to the dynamic analysis of propulsion reactors when the submarine is subjected to the effect of an underwater explosion.

Nuclear propulsion systems are composed of two main elements, namely the reactor (PWR type, which contains the nuclear core and produces the hot water for the primary loop) and the steam generator (in which heat exchanges between the primary and secondary loops take place, resulting in the production of steam conveyed in the engine). The present study is concerned with the dynamic behaviour of the reactor, which is sketched by Fig. 1 in a simplified manner. In pre-design stages, three-dimensional details of the geometry can be discarded in the analysis, so that a two-dimensional axi-symmetric model can be used in first approach. Figure 1 identifies two main parts of the reactor: the "outer structure" (pressure vessel) one the one hand, the "inner structure" (core supporting structure) on the other hand. The annular space comprised within these two structures is filled with the fluid of the primary

loop (pressurised water) and with various internal structures (hydraulic devices). At operating condition, the reactor is pressurised (P_o denoting the primary fluid pressure). The geometrical details of the reactor core are not accounted for in the present study (as will be made conspicuous in subsection 3, the core and internal pressurised fluid will only be modelled through their inertial effects). Using this engineering model of the reactor, it is then desired to evaluate the influence fluid-structure interaction effects (inertial, pre-stress, elastic/acoustic coupling, confinement, etc.) on the reactor dynamic behaviour when subjected to imposed acceleration and subsequently determine which effects are of engineering relevance. More precisely speaking, the study aims at answering the following key-questions [7,8]:

- What are the predominant coupling effects in the low frequency range (0–20 Hz), i.e. effects to be taken into account for the seismic analysis?
- What are the predominant coupling effects in the high frequency range (20–200 Hz), i.e. effects to account for in the shock analysis?
- What is the influence of the presence of internal structures as far as fluid-structure interaction is concerned?
- What is the influence of the static pressure P_o on the dynamic behaviour of the nuclear reactor?

With these questions in mind, the proposed study will be devoted to recalling various mathematical modelling of fluid-structure interactions in the case of the reactor (subsection 2), to performing the modal analysis of the nuclear pressure vessel (subsection 3) and to identifying the predominant FSI effects on the dynamic response of the system when subjected to seism or shock (subsection 4).

2. FLUID-STRUCTURE INTERACTION MODELLING WITHIN THE NUCLEAR REACTOR

2.1. PROBLEM DEFINITION AND GENERAL ASSUMPTIONS

Geometry of the problem is detailed in Fig. 1 above. Σ_k stands for the inner and outer structures ($k = 1$: inner structure, $k = 2$: outer structure), Ω for the fluid and Ω_S for the internal structures. In the industrial problem, the structure interface with the steam generator on the one hand, and the reactor supporting structure on the other hand, are rather complex. In the present simplified approach study, clamped conditions of the upper part of structures Σ_k are supposed to be representative of the stiffness interface of the reactor with the surrounding structures. $\partial\Sigma_{ko}$ denotes the boundary part of structure with imposed clamped conditions (see Fig. 1). Similarly, the fluid interface (reactor inlet and outlet for primary loop) are not accounted for in the simplified model: the fluid is then supposed to be confined within the inner and outer reactor structures. On the upper part of the reactor (denoted $\partial\Omega_\pi$ on Fig. 1), rigid wall conditions are assumed. In the 2D axi-symmetric model, a symmetry condition arises for the fluid problem on $r = 0$: the corresponding boundary of the fluid problem is then denoted $\partial\Omega_o$, and boundary conditions are also that of a rigid wall. On the other boundaries, structure and fluid are in contact: Γ_k denotes interface between fluid and structure Σ_k. On boundaries, the unit normal is $\mathbf{n}$ and points outward for the fluid domain and inward for the structure domains.

As the paper is concerned with the study of vibration of the coupled system and with the description of fluid-structure interaction, the dynamic of the fluid and structure will be described in the frame of linear elasticity. In addition, the modelling does not account for thickness of the inner and outer structures or for flow of fluid, in such manner that:

- Structure displacement $\mathbf{u}_k$, strain $\varepsilon(\mathbf{u}_k)$ and stress $\sigma(\mathbf{u}_k)$ fields will be described using an elastic shell model.

– Fluid pressure field p will be described using the potential flow model (when compressibility effects are discarded) or the acoustic wave propagation model (when fluid compressibility is accounted for).

Properties of fluid ρ_F (density), c (acoustic wave propagation velocity) and structure ρ_{Sk} (density), E_k (Young modulus) and v_k (Poisson coefficient) are calculated at temperature and pressure operating conditions.

As details of the reactor core are not thoroughly defined in pre-design stages, this latter is modelled with an equivalent inertia, using a mass element placed at the estimated position of the centre of gravity of the core.

As the numerical model aims at describing the confinement induced in the fluid domain by the structures, internal structures are accounted for in the analysis only through their geometry. Experiences gained from previous engineering studies on similar structures have shown that the additional stiffness and/or mass related to the internal structures could safely been neglected in comparison with the internal and external structures stiffness and mass.

Despite the various simplified assumptions listed above, the proposed reactor model is representative enough of the industrial structure so as to describe the fluid-structure coupling effects and to evaluate their relative importance in the context of a dynamic analysis.

2.2. ELASTIC STRUCTURE UNDER STATIC FLUID PRESSURE

At operating conditions, the nuclear reactor is pressurised and one open question from the engineering point of view is to know whether the modelling has to take effects of internal pressure loading into account, or not. The static pressure field induces pre-stress effect on the structure, whose description can be achieved within the following modelling frame [5]. Calculation of kinetic and potential energy of the structure subjected to inner static pressure field gives:

$$\varepsilon_{kin} = \frac{1}{2}\int_{\Sigma_k} \rho_k \left(\frac{\partial \mathbf{u}_k}{\partial t}\right)^2 d\Sigma_k \tag{1}$$

for the kinetic terms, and:

$$\varepsilon_{ela} = \frac{1}{2}\int_{\Sigma_k} \sigma_1(\mathbf{u}_k)\cdot\varepsilon_1(\mathbf{u}_k)d\Sigma_k + \frac{1}{2}\int_{\Sigma_k} \sigma_0(P_o)\cdot\varepsilon_2(\mathbf{u}_k)d\Sigma_k - \frac{1}{2}\int_{\Gamma_k} P_o\mathbf{n}_1\cdot\mathbf{u}d\Gamma_k \tag{2}$$

for the potential terms. $\varepsilon_1(\mathbf{u})$ stands for the linear part of the strain tensor, $\varepsilon_1(\mathbf{u})_{i,j} = \frac{1}{2}\left(\frac{\partial u_i}{\partial x_j} + \frac{\partial u_j}{\partial x_i}\right)$, and $\varepsilon_2(\mathbf{u})$ refers to the non linear part of the strain tensor, $\varepsilon_2(\mathbf{u})_{i,j} = \sum_k \frac{\partial u_i}{\partial x_k}\cdot\frac{\partial u_j}{\partial x_k}$. $\sigma_o(P_o)$ denotes the stress tensor due to static loading on the structure with pressure field P_o; $\mathbf{n}_1$ is the local normal vector calculated on the deformed static configuration under pressure loading. Equation (2) gives the potential energy with various terms:

– $\frac{1}{2}\int_{\Sigma_k} \sigma_1(\mathbf{u}_k)\cdot\varepsilon_1(\mathbf{u}_k)d\Sigma_k$ is the usual elastic linear terms which defines the linear stiffness matrix of the structure,

– $\frac{1}{2}\int_{\Gamma_k} P_o\mathbf{n}_1\cdot\mathbf{u}d\Gamma_k$ represents the geometric stiffness potential due to geometric variations of the normal vector **n** in the pressure field P_o,

– $\frac{1}{2}\int_{\Sigma_k} \sigma_0(P_o)\cdot\varepsilon_2(\mathbf{u}_k)d\Sigma_k$ accounts for pre-stress stiffness potential, taking into account pre-stress effects in the reference configuration.

A finite element discretisation of the variational principle for the elastic structure leads to the following matrix system:

$$\mathbf{M}_S\ddot{\mathbf{U}}(t)+[\mathbf{K}_S+P_o(\mathbf{K}_\sigma-\mathbf{K}_\pi)]\mathbf{U}(t)=0 \tag{3}$$

with $\mathbf{M}_S$ and $\mathbf{K}_S$ the structure mass and stiffness matrices. As expressed by Eq. (3), the effect of a pressure loading is modelled with the added stiffness matrix K_σ–K_π.

2.3. ELASTIC STRUCTURE COUPLED WITH INCOMPRESSIBLE FLUID

As stated above, the reactor behaviour is described in the frame of linear elasticity. The structure problem in the frequency domain reads[1]:

$$-\rho_S\omega^2 u_{k,i}-\frac{\partial\sigma_{ij}(\mathbf{u}_k)}{\partial x_{ij}}=0 \quad \text{in } \Sigma_x \tag{4}$$

with boundary condition:

$$\mathbf{u}_k = 0 \text{ on } \partial\Sigma_{ko} \tag{5}$$

When the frequency range of interest does not exceed a few ten Hertz and when the typical size of the system is a few meters, the fluid can safely be modelled as incompressible [4]. In addition, since the fluid in the reactor is not so highly confined as to induce large viscous effects, it can be assumed inviscid. Accordingly, the fluid problem is described by the potential flow model, which reads:

$$\frac{\partial^2 p}{\partial x_i^{\,2}}=0 \quad \text{in } \Omega \tag{6}$$

$$\frac{\partial p}{\partial x_j}\cdot n_j=0 \quad \text{on } \partial\Omega_\pi \text{ and } \partial\Omega_o \tag{7}$$

[1]An identical set of equation is written for each structure, i.e. k = 1,2 in what follows.

Coupling between fluid and structure problems is modelled with the following conditions:

$$\sigma_{ij}(\mathbf{u}_k)\cdot n_j = -pn_i \text{ on } \Gamma_k \tag{8}$$

$$\frac{\partial p}{\partial x_i}\cdot n_i = \rho_F \omega^2 \mathbf{u}_k \cdot \mathbf{n} \text{ on } \Gamma_k \tag{9}$$

Equation (8) expresses the continuity of the normal component of the stress tensor at the fluid-structure interface. On Γ_k, the fluid acts on the structure via an imposed pressure that creates a structure loading in the normal direction at the structure boundary . Equation (9) expresses the continuity of the displacement normal component. On Γ_k, the structure acts on the fluid via an imposed displacement in the normal direction at the fluid boundary.

Numerical resolution of the coupled problem is obtained with the finite element method, starting with the variationnal formulation of the fluid-structure interaction problem. On the one hand, the structure problem is written as:

$$-\omega^2 \int_{\Sigma_k} \rho_{Sk}\mathbf{u}_k \cdot \delta\mathbf{u}_k d\Sigma_k + \int_{\Sigma_k} \sigma_{ij}(\mathbf{u}_k)\varepsilon_{ij}(\delta\mathbf{u}_k)d\Sigma_k - \int_{\Gamma_k} p\mathbf{n}\cdot\delta\mathbf{u}_k d\Gamma_k = 0 \tag{10}$$

for any virtual displacement field $\delta\mathbf{u}_k$ which complies with boundary condition (5). On the other hand, the fluid problem is written:

$$-\rho_F\omega^2 \int_{\Gamma_k} \mathbf{u}_k\cdot\mathbf{n}\delta p d\Gamma_k + \int_{\Omega} \frac{\partial p}{\partial x_i}\frac{\partial \delta p}{\partial x_i} d\Omega = 0 \tag{11}$$

for any virtual pressure field δp satisfying boundary condition (7).

Spatial discretisation of the weak formulations (10) and (11) is performed with finite elements [6]. Mass and stiffness matrices of the fluid and structure problem arise from the finite element discretisation:

$$\int_{\Sigma_k} \rho_{Sk}\mathbf{u}_k\cdot\delta\mathbf{u}_k d\Sigma_k \rightarrow \delta\mathbf{U}_k{}^T\mathbf{M}_{Sk}\mathbf{U}_k \tag{12}$$

$$\int_{\Sigma_k} \sigma_{ij}(\mathbf{u}_k)\varepsilon_{ij}(\delta\mathbf{u}_k)d\Sigma_k \rightarrow \delta\mathbf{U}_k{}^T\mathbf{K}_{Sk}\mathbf{U}_k \tag{13}$$

$$\int_{\Omega} \frac{\partial p}{\partial x_i}\frac{\partial\delta p}{\partial x_i} d\Omega \rightarrow \delta\mathbf{P}^T\mathbf{K}_F\mathbf{P} \tag{14}$$

Fluid-structure interaction matrices are used to discretise the coupled terms and are defined as:

$$\int_{\Gamma} p\mathbf{n}\cdot\delta\mathbf{u}_k d\Gamma_k \rightarrow \delta\mathbf{U}_k{}^T\mathbf{R}_k\mathbf{P} \qquad \int_{\Gamma_k} \mathbf{u}_k\cdot\mathbf{n}\delta p d\Gamma_k \rightarrow \delta\mathbf{P}^T\mathbf{R}_k{}^T\mathbf{U}_k \tag{15}$$

Finite element discretisation of Eqs. (10) and (11) is then:

$$-\omega^2 \mathbf{M}_S \mathbf{U}(\omega) + \mathbf{K}_S \mathbf{U}(\omega) = \mathbf{R}\mathbf{P}(\omega) \tag{16}$$

$$\mathbf{K}_F \mathbf{P}(\omega) = \rho_F \omega^2 \mathbf{R}^T \mathbf{U}(\omega) \tag{17}$$

Pressure can be calculated from (17) and substituted in (16), yielding:

$$-\omega^2 (\mathbf{M}_S + \rho_F \mathbf{R}\mathbf{K}_F^{-1}\mathbf{R}^T)\mathbf{U}(\omega) + \mathbf{K}_S \mathbf{U}(\omega) = \mathbf{0} \tag{18}$$

Equation (18) describes the structure dynamic with fluid-structure interaction represented through the so-called added mass operator $\mathbf{M}_H$ defined as:

$$\mathbf{M}_H = \rho_F \mathbf{R}\mathbf{K}_F^{-1}\mathbf{R}^T \tag{19}$$

The added mass matrix is positive definite: as a well know result, eigenfrequencies of the structure with fluid are lower than the eigenfrequencies of the structure without fluid. This inertial effect is increased in the case of confined fluid [9]. In the general case, the added matrix is not diagonal: coupling between structure modes can then be expected in presence of fluid.

Static pressure loading and fluid-structure interaction can both be accounted for: in such case, the structure eigenmodes are P_o-dependant and are the solutions of the eigenvalue problem:

$$-\omega^2 (\mathbf{M}_S + \rho_F \mathbf{R}\mathbf{K}_F^{-1}\mathbf{R}^T)\mathbf{U}(\omega, P_o) + (\mathbf{K}_S + P_o(\mathbf{K}_\sigma - \mathbf{K}_\pi))\mathbf{U}(\omega, P_o) = \mathbf{0} \tag{20}$$

2.4. ELASTIC STRUCTURE COUPLED WITH COMPRESSIBLE FLUID

For higher frequency analysis, the fluid can no longer be considered as incompressible. The fluid pressure field satisfies the acoustic wave propagation equation which reads:

$$-\frac{\omega^2}{c^2} p - \frac{\partial^2 p}{\partial x_i^{\,2}} = 0 \tag{21}$$

in the frequency domain. Coupling condition with the structure vibration at the fluid-structure interface remains unchanged. Using the test function method, the weak formulation of the fluid problem with structure coupling is:

$$-\omega^2 \int_\Omega \frac{p\delta p}{c^2} d\Omega - \rho_F \omega^2 \int_{\Gamma_k} \mathbf{u}_k \cdot \mathbf{n} \delta p d\Gamma_k + \int_\Omega \frac{\partial p}{\partial x_i} \frac{\partial \delta p}{\partial x_i} d\Omega = 0 \tag{22}$$

Finite element discretisation of the compressibility term yields the fluid mass matrix $\mathbf{M}_F$:

$$\int_\Omega \frac{p\delta p}{c^2} d\Omega \rightarrow \delta \mathbf{P}^T \mathbf{M}_F \mathbf{P} \tag{23}$$

Finally, the coupled problem takes the following form:

$$\begin{bmatrix} \mathbf{K}_S & -\mathbf{R} \\ \mathbf{0} & \mathbf{K}_F \end{bmatrix} \begin{Bmatrix} \mathbf{U}(\omega) \\ \mathbf{P}(\omega) \end{Bmatrix} = \omega^2 \begin{bmatrix} \mathbf{M}_S & \mathbf{0} \\ \rho_F \mathbf{R}^T & \mathbf{M}_F \end{bmatrix} \begin{Bmatrix} \mathbf{U}(\omega) \\ \mathbf{P}(\omega) \end{Bmatrix} \tag{24}$$

Equation (24) involves non-symmetric mass and stiffness matrices. Although the eigenvalues of the coupled problem can be obtained with a non-symmetric algorithm [10], this formulation does not allow a direct computation of participation factors and effective masses, which are requested for dynamic analysis with modal methods (see subsection 4). Furthermore, non-symmetric algorithms require higher computational time as symmetric ones. From that point of view, the use of symmetric coupled formulations is still nowadays a key-issue for engineering applications [11].

Many authors have proposed alternative approaches in order to obtain a symmetric coupled problem [12,13]. In the present study, the coupled problem is formulated using the ($\mathbf{u}$, p, φ) coupled variable [14,15], in which the structure problem is formulated in terms of displacement ($\mathbf{u}$) and the fluid problem in terms of pressure (p) and displacement potential (φ). Pressure and displacement potential in the fluid domain are related by:

$$p = \rho_F \omega^2 \varphi \tag{25}$$

Equation (25) can be written as follows, using the fluid mass matrix:

$$-\omega^2 \mathbf{M}_F \Phi(\omega) + 1/\rho_F \mathbf{M}_F \mathbf{P}(\omega) = \mathbf{0} \tag{26}$$

Combining Eq. (26) together with Eq. (24) leads to the following system, which involves symmetric mass and stiffness matrices:

$$\begin{bmatrix} \mathbf{K}_S & \mathbf{0} & \mathbf{0} \\ \mathbf{0} & 1/\rho_F \mathbf{M}_F & \mathbf{0} \\ \mathbf{0} & \mathbf{0} & \mathbf{0} \end{bmatrix} \begin{Bmatrix} \mathbf{U}(\omega) \\ \mathbf{P}(\omega) \\ \Phi(\omega) \end{Bmatrix} = \omega^2 \begin{bmatrix} \mathbf{M}_S & \mathbf{0} & \rho_F \mathbf{R} \\ \mathbf{0} & \mathbf{0} & \mathbf{M}_F \\ \rho_F \mathbf{R}^T & \mathbf{M}_F & -\rho_F \mathbf{K}_F \end{bmatrix} \begin{Bmatrix} \mathbf{U}(\omega) \\ \mathbf{P}(\omega) \\ \Phi(\omega) \end{Bmatrix} \tag{27}$$

It is worth discussing here the physical interpretation of the various matrices defined above. The structure kinetic and elastic energy are calculated according to:

$$\varepsilon^s_{kin} = \frac{\omega^2}{2} \mathbf{U}^T \mathbf{M}_S \mathbf{U} \qquad \varepsilon^s_{ela} = \frac{1}{2} \mathbf{U}^T \mathbf{K}_S \mathbf{U} \tag{28}$$

Structure kinetic energy is evaluated with the mass matrix and potential energy with the stiffness matrix.

The fluid problem is formulated here in a dual formulation and it can be shown that the fluid kinetic and elastic energy are calculated as:

$$\varepsilon^f_{kin} = \frac{1}{2\omega^2} \mathbf{P}^T \mathbf{K}_F / \rho_F \mathbf{P} \qquad \varepsilon^f_{ela} = \frac{1}{2} \mathbf{P}^T \mathbf{M}_F / \rho_F \mathbf{P} \tag{29}$$

Fluid kinetic energy is now evaluated with the "stiffness matrix", as defined by Eq. (14), and potential energy with the "mass matrix", as defined by Eq. (23). This denomination, though questionable from the energy point of view, is used in order to gather the stiffness

matrices $\mathbf{K}_S$ and $\mathbf{K}_F$ in the "stiffness term" and the mass matrices $\mathbf{M}_S$ and $\mathbf{M}_F$ in the "mass term" of the coupled problem, see Eq. (24) above.

2.5. ELASTIC STRUCTURE AND SOLID INCLUSIONS COUPLED WITH FLUID

Fluid-structure interaction modelling presented in the preceding subsections can be applied to the industrial problem under study here. However, a complete modelling of the geometrical details of the inner structures of the nuclear reactor would be based on a three-dimensional finite element model, hence requiring high modelling and computational effort. From the engineering standpoint, a 2D axi-symmetric model of industrial structures is of convenient use in pre-design analysis. It is then desired to develop a numerical method that accounts for fluid confinement effects without using a full 3D model of the nuclear reactor. Modelling of the inner structure can be achieved in that context with a homogenisation technique [16].

The general principle of the proposed method can be described by Fig. 2, in the case of two concentric cylinders coupled by a fluid, which can be viewed as a 2D representation of the industrial problem. The internal structures are modelled as rigid cylinders within the annular space between the inner and outer cylinder; the rigid structures are linked to the inner cylinder. Modelling fluid-structure interaction and accounting for the internal structures can be performed:

- Either by using a numerical model that describes the geometry of the inclusions within the fluid annular space, as represented by Fig. 2, case (a). In such case, added mass and confinement effects are directly described with the numerical method used in the former case.
- Or by an equivalent fluid model that takes into account the added mass and confinement effects through an equivalent fluid model. Fluid-structure interaction effects are then described in an indirect, though powerful, way because in this latter case, detailed geometry of the solid inclusion do not need meshing, see Fig. 2, case (b). Such an approach is based on the application of homogenisation methods, which lies on the geometrical periodicity of problem.

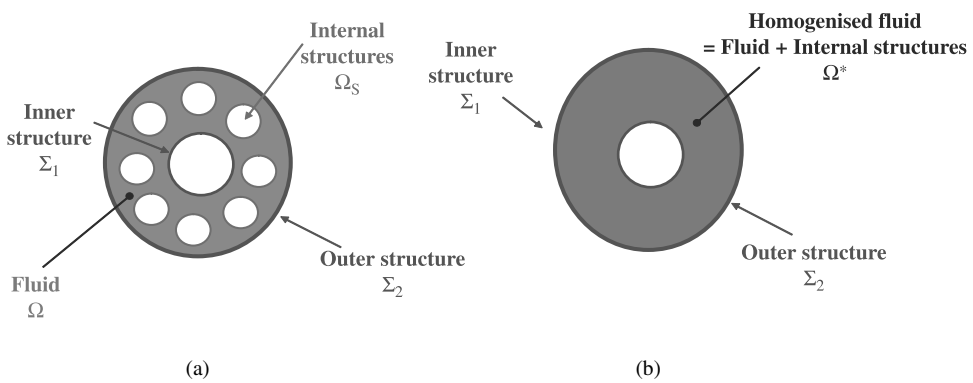

Figure 2 Two concentric cylinders coupled with a fluid embedded in an annular space. (a) With solid inclusions modelling. (b) With equivalent homogenised fluid and inclusions modelling.

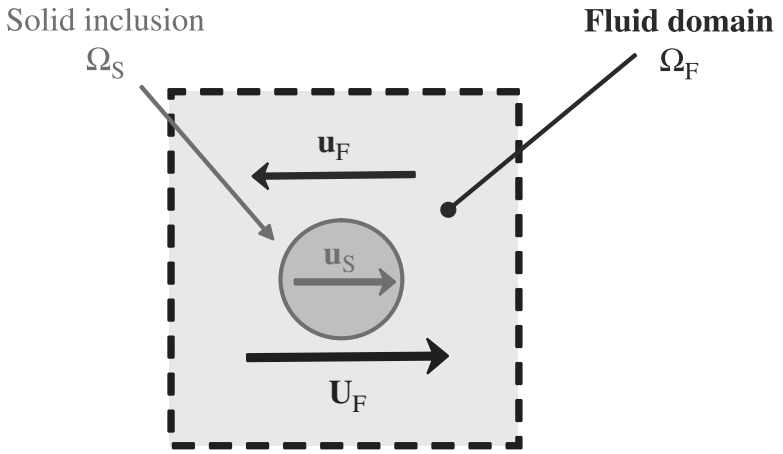

Figure 3 Elementary cell: solid inclusion in quiescent fluid.

Homogenisation methods have been developed and applied in various fields for structures with periodic geometry [17] or for fluids in porous media [18]. Such methods have also been applied to fluid-structure interaction problems [19] in particular in power nuclear engineering for FSI modelling in tube bundle [20,21], heat exchangers [22] or reactor cores [23,24,25]. In the present study, application of homogenisation methods for fluid-structure interaction modelling in the case of pressure vessel internals is presented. To the author's knowledge, this kind of application has not been reported in the literature. It differs from the previous cases at least from the following points of view:

– The number of inclusions in the pressure vessel is much lower than in tube bundle (about 30 internal structures in the former case, more than 5000 tubes in the latter case).
– The geometry of the problem is characterised by a cylindrical confinement within an annular space, whereas confinement in nuclear cores is rather of square-in-square type.

In the industrial case under consideration in the present paper, the inner and outer shell radius and the number of inclusions within the pressure vessel are such that one can model each fluid cell as a square with inner inclusion as a circle, see Fig. 3.

For each cell, Ω_S denotes the rigid solid domain, Ω_F the fluid domain and $\Omega_T = \Omega_S \cup \Omega_F$ the total cell domain. $\mathbf{u}_S$ is the rigid inclusion displacement, $\mathbf{u}_F$ the fluid displacement field (for local description) and $\mathbf{U}_F$ the average fluid displacement (for global description), defined as the average value of the displacement (solid and fluid) over the total domain (solid and fluid):

$$\mathbf{U}_F = \frac{|\Omega_S|}{|\Omega_T|}\mathbf{u}_S + \frac{1}{|\Omega_T|}\int_{\Omega_F} \mathbf{u}_F d\Omega_F \tag{30}$$

On the homogenised fluid domain, the pressure field p is calculated from the average fluid acceleration field and the solid acceleration according to:

$$-\rho_F \omega^2 \mathbf{U}_F = -(1-J)\nabla p - \rho_F J \omega^2 \mathbf{u}_S \tag{31}$$

The confinement ratio is such that $J \in [0,1]$. It is worth emphasising the asymptotic cases $J = 0$ and $J = 1$, which respectively correspond to the following situations:

- $J = 0$ when there are no solid inclusions. In that case, Eq. (31) then yields the usual relation between pressure and acceleration, i.e. $-\rho_F \omega^2 \mathbf{U}_F = \nabla p$.
- $J = 1$ is a limit case where there is no fluid in Ω_T. In that case Eq. (31) reads $\mathbf{U}_F = \mathbf{u}_S$, which is physically consistent: the elementary cell is a solid structure cell.

The first term in the right hand side of Eq. (31) is the pressure gradient ∇p, corrected with the $1 - J$ coefficient which takes into account the presence of the solid inclusions in the fluid cell. Equation (31) states that for a given fluid motion, the pressure gradient is increased with the confinement, which is a typical effect of the geometrical confinement.

On the other hand, the homogenised fluid state equation reads:

$$p = -\rho_F c^2 \nabla \cdot \mathbf{U}_F \tag{32}$$

Combining Eqs. (31) and (32) yields:

$$\frac{\omega^2}{c^2} + (1 - J)\Delta p = 0 \quad \text{on } \Omega^* \tag{33}$$

where Ω^* is the homogenised fluid domain. Boundary conditions (rigid wall or symmetry condition) are:

$$\frac{\partial p}{\partial n} = 0 \ \text{ on } \partial\Omega_o^*, \ \frac{\partial p}{\partial n} = 0 \ \text{ on } \ \partial\Omega_\pi^* \tag{34}$$

and the coupling condition with the structure problem is:

$$\frac{\partial p}{\partial n} = -\rho_F \omega^2 \mathbf{u}_k \cdot \mathbf{n} \ \text{ on } \Gamma_k \tag{35}$$

which is equivalent to:

$$\mathbf{U}_F \cdot \mathbf{n} = \mathbf{u}_k \cdot \mathbf{n} \ \text{ on } \Gamma_k \tag{36}$$

The variationnal formulation of the fluid problem is written using the test function method, and taking the cinematic condition $\mathbf{u}_S \equiv \mathbf{u}_1$ on Γ_1 into account (inner inclusions are rigidly linked to the inner shell). The following formulation is finally obtained:

$$\begin{aligned} &-\omega^2 \int_{\Omega^*} \frac{p\delta p}{c^2} d\Omega^* + \int_{\Omega^*} (1 - J)\nabla p \cdot \nabla \delta p d\Omega^* = \omega^2 \int_{\Gamma_1} \rho_F (1 - J)\mathbf{u}_1 \cdot \mathbf{n}\delta p d\Gamma_1 \\ &+\omega^2 \int_{\Gamma_2} \rho_F \mathbf{u}_2 \cdot \mathbf{n}\delta p d\Gamma_2 + \omega^2 \int_{\Gamma_2} \rho_F J\mathbf{u}_1 \cdot \mathbf{n}\delta p d\Gamma_2 \end{aligned} \tag{37}$$

The structure problem is described according to the linear elasticity theory for each system Σ_k:

$$-\omega^2 \rho_{Sk} u_{k,i} - \frac{\partial \sigma_{ij}(\mathbf{u}_k)}{\partial x_j} = \delta_{k,1} \left(\int_{\Omega_*} d \right) \cdot \mathbf{e}_i \tag{38}$$

where $\delta_{k,1} = 1$ (for $k = 1$), $\delta_{k,1} = 0$ (for $k = 2$). The dynamic equation of the inner shell Σ_1 takes into account the forces exerted on the solid inclusions by the fluid. From a local analysis in the elementary fluid cell, one can write the fluid force acting on a single solid inclusion. From the global point of view, the equivalent fluid force density $d\tilde{\mathbf{o}}$ is derived [16]:

$$d\tilde{o} = \left(-J \nabla p - \rho_F I \frac{|\Omega_F|}{|\Omega_T|} \ddot{\mathbf{u}}_S \right) d\Omega^* \tag{39}$$

with I calculated from J according to $J = \frac{|\Omega_S|}{|\Omega_T|} + I \frac{|\Omega_F|}{|\Omega_T|}$.

Boundary conditions are (5) and coupling condition with the fluid is (8). The variationnal formulation of the structure problem reads:

$$\begin{aligned} &-\omega^2 \int_{\Sigma_k} \rho_{Sk} \mathbf{u}_k \cdot \delta \mathbf{u}_k d\Sigma_k + \int_{\Sigma_k} \sigma_{ij}(\mathbf{u}_k) \varepsilon_{ij}(\delta \mathbf{u}_k) d\Sigma_k = \\ &\int_{\Gamma_1} p(1-J) \mathbf{n} \cdot \delta \mathbf{u}_1 d\Gamma_1 + \int_{\Gamma_2} p \mathbf{n} \cdot \delta \mathbf{u}_2 d\Gamma_2 + \omega^2 \tilde{m}_1 \times \mathbf{u}_1 \cdot \delta \mathbf{u}_1 + \int_{\Gamma_2} -Jp \mathbf{n} \cdot \delta \mathbf{u}_1 d\Gamma_2 \end{aligned} \tag{40}$$

with $\tilde{m}_1 = \int_{\Omega^*} \rho_F I \frac{|\Omega_F|}{|\Omega_T|} d\Omega^*$.

Finite element discretisation of Eqs. (37) and (40) yields:

$$\begin{bmatrix} \mathbf{K}_S^1 & \mathbf{0} & -(1-J)\mathbf{R}_1 + J\mathbf{H} \\ \mathbf{0} & \mathbf{K}_S^2 & \mathbf{R}_2 \\ \mathbf{0} & \mathbf{0} & (1-J)\mathbf{K}_F \end{bmatrix} \begin{Bmatrix} \mathbf{U}_1(\omega) \\ \mathbf{U}_2(\omega) \\ \mathbf{P}(\omega) \end{Bmatrix} = \omega^2 \begin{bmatrix} \mathbf{M}_S^1 + \tilde{\mathbf{M}}_1 & \mathbf{0} & \mathbf{0} \\ \mathbf{0} & \mathbf{M}_S^2 & \mathbf{0} \\ \rho_F (1-J)\mathbf{R}_1^T - J\mathbf{H}^T & \rho_F \mathbf{R}_2^T & \mathbf{M}_F \end{bmatrix} \begin{Bmatrix} \mathbf{U}_1(\omega) \\ \mathbf{U}_2(\omega) \\ \mathbf{P}(\omega) \end{Bmatrix} \tag{41}$$

Equation (41) involves various operators, which have been defined in the previous subsection, as well as specific operators, namely:

– Added mass operator $\tilde{\mathbf{M}}_1$

$$\int_{\Omega^*} \rho_F I \frac{|\Omega_F|}{|\Omega_T|} d\Omega^* \times \ddot{\mathbf{u}}_1 \cdot \delta \mathbf{u}_1 \rightarrow \delta \mathbf{U}_1^T \tilde{\mathbf{M}}_1 \mathbf{U}_1 \tag{42}$$

– Coupling operator $\mathbf{H}$

$$\int_{\Gamma_2} p \mathbf{n} \cdot \delta \mathbf{u}_1 d\Gamma \rightarrow \delta \mathbf{U}_1 \mathbf{H} \mathbf{P} \tag{43}$$

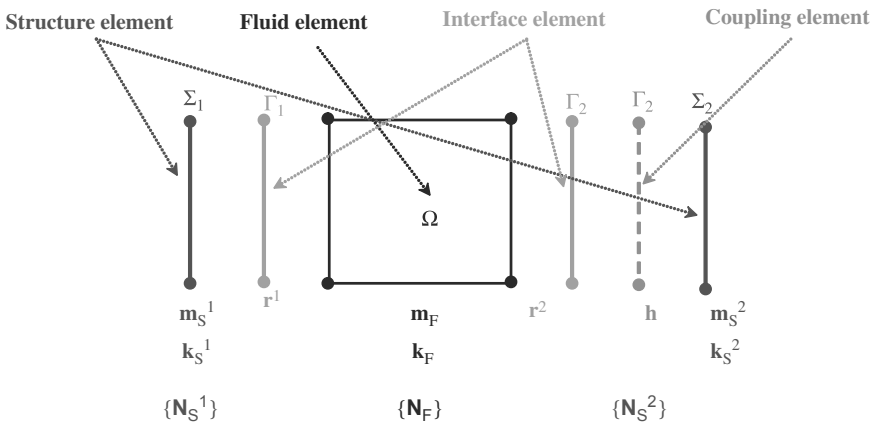

Figure 4 Fluid and structure finite elements, coupling and interface elements

The elementary fluid and structure matrices are calculated on fluid and structure finite elements with the fluid and structure shape functions $\left\{N_S^k\right\}$ and $\{\mathrm{N}_F\}$. The elementary interaction matrices are calculated with interface elements (see Fig. 4) using the shape functions of the structure and fluid problem. The coupling matrix **H** is assembled with elementary matrices, calculated on Γ_2 with a coupling element using the shape functions $\left\{N_S^1\right\}$ and $\{\mathrm{N}_F\}$.

The coupled formulation given by Eq. (41) is of the same type that the non-symmetric (**u**,p) formulation, with corrections on the fluid stiffness matrix and on the fluid-structure coupling matrix. An equivalent symmetric formulation of Eq. (41) can be derived using the (**u**,p,φ) variables (see previous subsection).

The proposed homogenisation method lies on the calculation of the confinement ratio J, which can be estimated using a straightforward method [26]. Fluid forces acting on a rigid inclusion Ω_S moving in an elementary fluid cell Ω_F are calculated as:

$$\mathbf{\Phi} = -m_h \ddot{\mathbf{u}}_S + (m_h + m_d)\ddot{\mathbf{U}}_F \tag{44}$$

where m_h is the fluid added mass and $m_d = \rho_F \left|\Omega_S\right|$ is the inclusion displaced mass. On the other hand, external force acting on the fluid is calculated as $-\left|\Omega_T\right|\nabla p - \mathbf{\Phi}$, hence:

$$\int_{\Omega_F} \rho_F \ddot{\mathbf{u}}_F d\Omega_F = -\left|\Omega_T\right|\nabla p + m_h \ddot{\mathbf{u}}_S - (m_h + \rho_F \left|\Omega_S\right|)\ddot{\mathbf{U}}_F \tag{45}$$

Taking into account Eq. (30), the previous equation is reformulated:

$$\left(\rho_F \left(\left|\Omega_T\right| + \left|\Omega_S\right|\right) + m_h\right)\ddot{\mathbf{U}}_F = -\left|\Omega_T\right|\nabla p + (m_h + \rho_F \left|\Omega_S\right|)\,\ddot{\mathbf{u}}_S \tag{46}$$

Whence:

$$\rho_F \ddot{\mathbf{U}}_F = -(1-J)\nabla p + J\,\rho_F \ddot{\mathbf{u}}_S \tag{47}$$

which is Eq. (31). Combining Eqs. (46) and (47) yields:

$$J = (m_h + \rho_F |\Omega_S|) / \left(m_h + \rho_F (|\Omega_T| + |\Omega_S|)\right) \tag{48}$$

which is an alternate definition of J. Computation of coefficient J is performed with Eq. (48), using an elementary cell calculation in order to evaluate the added mass term m_h. This latter is then calculated assuming that the inner inclusion is a rigid system of mass m and stiffness k. Comparing the system eigenpulsation in vacuum $\omega_o = \sqrt{\frac{k}{m}}$ and the eigenpulsation in fluid $\omega_h = \sqrt{\frac{k}{m+m_h}}$ yields the added mass m_h.

It is also important to stress that the proposed method is proved to be physically conservative in terms of total mass description [16]: effective masses can be calculated for each coupled eigenmode and the cumulated effective masses give the total mass of the system (fluid and structure), such a property being of paramount importance for the dynamic analysis using modal methods (see subsection 4).

3. MODAL ANALYSIS OF THE NUCLEAR REACTOR WITH FLUID-STRUCTURE INTERACTION

3.1. FINITE ELEMENT MODEL OF THE NUCLEAR REACTOR

The present analysis is based on a simplified model of the nuclear reactor in which 3D geometrical details have not been accounted for: in pre-design stages, a 2D axi-symmetric representation of the reactor is representative enough of the global behaviour of the structure (see subsection 2 and Fig. 1).

In 2D axi-symmetric modelling, the problem unknowns, namely the structure displacement and fluid pressure and displacement potential ($\mathbf{u}$, p, φ), are periodic functions of the angular variable θ. As the dynamic loading is imposed in a transverse direction with respect to the vertical axis of the structure, it is not purely axi-symmetric. Accordingly, it is suited to use a Fourier expansion of fields ($\mathbf{u}$, p, φ):

$$\begin{Bmatrix} u_r(r,\theta,z) \\ u_\theta(r,\theta,z) \\ u_z(r,\theta,z) \\ p(r,\theta,z) \\ \varphi(r,\theta,z) \end{Bmatrix} = \begin{Bmatrix} u_r{}^0(r,z) \\ u_\theta{}^0(r,z) \\ u_z{}^0(r,z) \\ p^0(r,z) \\ \varphi(r,\theta,z) \end{Bmatrix} + \sum_{s\geq 1} \begin{Bmatrix} u_r{}^s(r,z) \\ u_\theta{}^s(r,z) \\ u_z{}^s(r,z) \\ p^s(r,z) \\ \varphi^s(r,\theta,z) \end{Bmatrix} \cdot cos(s\,\theta) + \sum_{a\geq 1} \begin{Bmatrix} u_r{}^a(r,z) \\ -u_\theta{}^a(r,z) \\ u_z{}^a(r,z) \\ p^a(r,z) \\ \varphi^a(r,\theta,z) \end{Bmatrix} \cdot sin(a\,\theta) \tag{49}$$

which exhibits pure axi-symmetric modes with no θ-dependency (represented by the upper script 0), symmetric modes (denoted by $s \geq 1$) and anti-symmetric modes (denoted by $a \geq 1$). The modes of interest here (seismic modes) are the symmetric and anti-symmetric modes of order one ($s = 1$, $a = 1$).

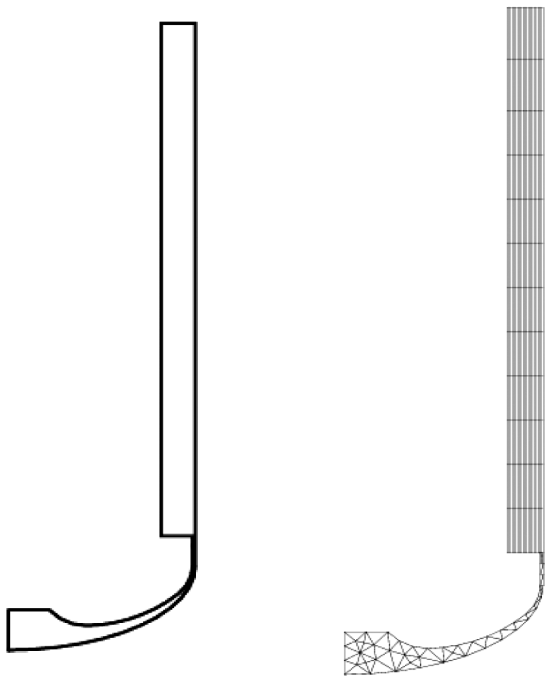

Figure 5 Axi-symmetric model of the nuclear pressure vessel and finite element mesh of the inner fluid.

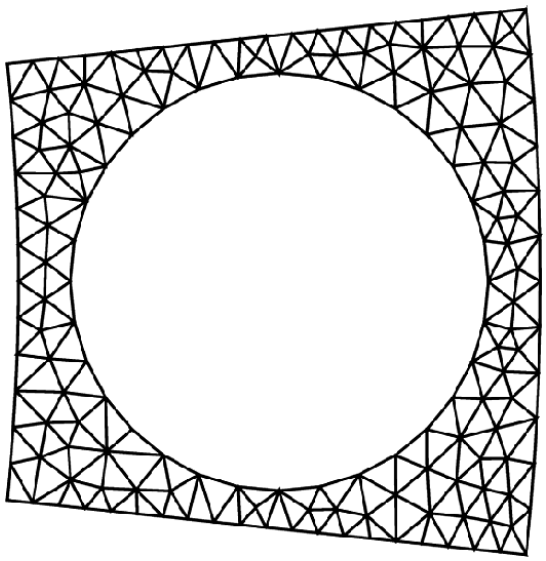

Figure 6 Elementary cell mesh for confinement ratio calculation.

The CASTEM code [27] is used to produce the finite element model of the coupled problem (see Fig. 5), using:

- 1D axi-symmetric shell linear elements for the structure problem;
- 2D axi-symmetric acoustic linear elements for the fluid problem.

Table 1 Confinement coefficient J for the various zones in the reactor

Zone #	Confinement coefficient J
1	0.57
2	0.45
3	0.34
4	0.24
5	0.15
6	0.13
7	0.23
8	0.62
9	0.62
10	0.44

Table 2 Reactor eigenfrequencies (in Hz) and effective masses (in % of total mass) using various fluid-structure modelling

Fuid-structure modelling	Mode #1	Mode #2	Mode #3
w/o. fluid	43.8 Hz – 39.2%	102.7 Hz – 25.3 %	138.3 Hz – 9.6%
w. fluid (incompressible)	25.7 Hz – 3.1%	79.0 Hz – 65.6%	102.0 Hz – 1.0%
w. fluid (incompressible) + static pressure P_o	26.0 Hz – 3.2%	79.4 Hz – 65.5%	102.3 Hz – 1.1%
w. fluid (compressible)	27.2 Hz – 3.9%	78.8 Hz – 61.8%	94.6 Hz – 4.6 %
w. fluid and internal structures	21.3 Hz – 2.8%	64.8 Hz – 70.1%	82.7 Hz – 1.5%

Modelling of geometrical confinement induced by internal structures requires the computation of the confinement ratio J. This is achieved through an elementary cell calculation model (see subsection 2). The annular space between the reactor inner and outer structures is divided in ten zones (from bottom to top), describing the vertical variation of the confinement. Figure 6 gives an example of elementary cell mesh which enables the calculation of the added mass term in Eq. (46). Table 1 gives the corresponding values of the confinement ratio in the various zones of the reactor.

3.2. MODAL ANALYSIS WITH FLUID-STRUCTURE INTERACTION MODELLING

Modal analysis of the nuclear reactor can now be performed, using the various fluid modelling presented in the preceding subsections. Eigenfrequencies and effective masses of the system are gathered in Tab. 2.

3.2.1. Structure without fluid

Calculation is first performed for the structure alone, i.e. without any fluid coupling. Figure 7 shows the first two eigenmodes of the system. The first mode (43.8 Hz) is a bending mode of the inner structure, the second mode (102.7 Hz) is a bending mode of the outer structure. The cumulated modal mass for these two modes represents up to 66% of the total structure mass. More than 85% of the total mass can be taken into account with the three subsequent modes.

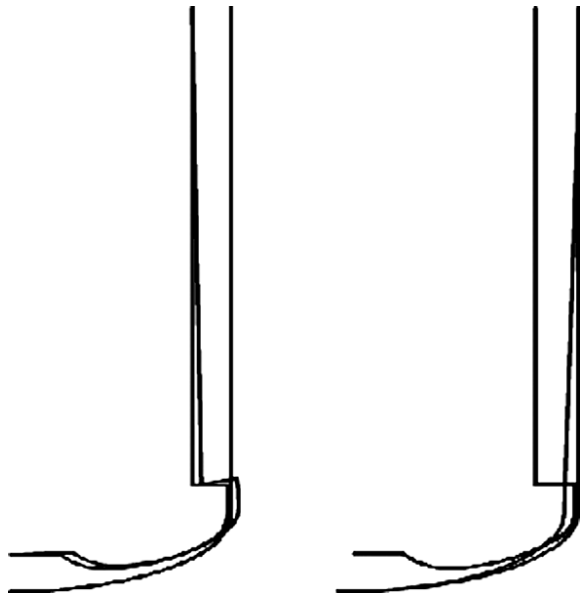

Figure 7 Eigenmode shapes of the reactor without fluid coupling.

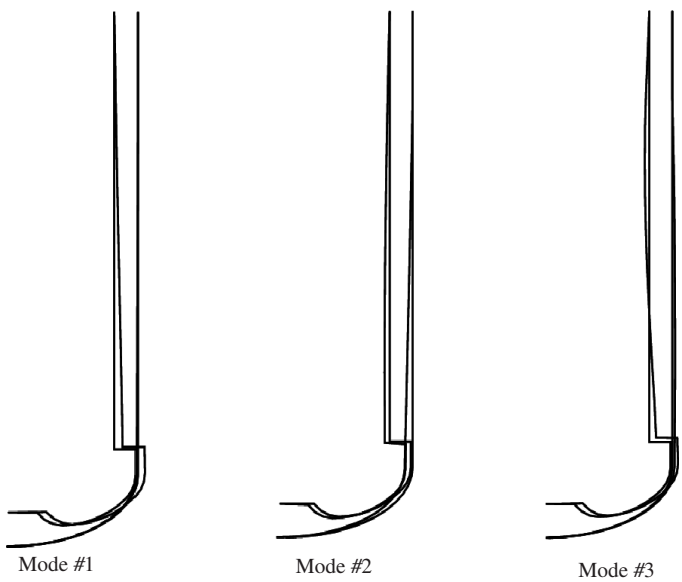

Figure 8 Eigenmode shapes of the reactor coupled with fluid.

3.2.2 Structure coupled with incompressible fluid

Eigenfrequencies and effective masses of the reactor with fluid coupling (without internal structure modelling) using an incompressible fluid model are then calculated; Fig. 8 gives a representation of the first three eigenmodes.

The first coupled mode is a bending mode of the inner structure coupled with the fluid; the frequency is lowered from 43.8 Hz to 25.7 Hz, as a result of inertial effects of the fluid. The second and third modes are coupled bending modes of the inner and outer structure at frequency 79.0 Hz (in phase bending mode) and 102.0 Hz (phase opposition bending mode) respectively: frequencies of the modes are lowered (inertial effect) and bending modes of the inner and outer structure are coupled (coupling effects).

Furthermore, the effective masses of the coupled mode differ significantly from that of the uncoupled modes. While in the latter case, the first two modes represent about 40% and 30% of the total mass respectively, in the former case, the first mode only accounts for 3% of the system mass and the second mode for more than 60% of the total mass.

These results clearly highlight the influence of fluid-structure coupling on the dynamic of the reactor: the eigenmode shapes, frequencies and effective masses are dramatically different when fluid coupling is accounted for. Consequences on the reactor response to seism or shock of fluid-structure interaction are detailed in the next subsection.

3.2.3. Structure coupled with incompressible fluid with static pressure

Static pressure loading does not induce significant changes in the system behaviour: as a result of pre-stress effect, global stiffness of the reactor increases, but the influence remains negligible for an extended range of pressure. Eigenmode shapes are not changed, eigenfrequencies as slightly raised, and effective masses are identical, when compared with calculation without static fluid pressure effects.

Such a result could have been expected a priori because the pressure vessel is designed in order to fulfil current regulation in terms of static pressure resistance. However, the coupled calculation with inner pressure correction terms demonstrates that static (pressure resistance) and dynamic (modal analysis with fluid-structure interaction) design can be performed separately as it is indeed current practice in design office.

3.2.4. Structure coupled with compressible fluid

Influence of fluid compressibility is much more significant, for modes above 100 Hz. The first two coupled eigenmodes are slightly affected by fluid compressibility: their frequency and effective mass are roughly the same as that computed with the incompressible fluid model the (27.2 Hz, 3.95% of the total mass and 78.8 Hz, 61.7% respectively obtained with the compressible fluid model, versus 26.2 Hz, 3.13% and 78.5 Hz, 65.6% obtained with the incompressible fluid model). The third coupled mode is more affected by fluid compressibility: as a result of elasto-acoustic coupling, its frequency is lowered to 94.6 Hz (to be compared with 102.3 Hz in the incompressible case) and its effective mass is increased up to 4.65% (to be compared with 1.1% in the incompressible case).

As pointed out by several authors, the modal analysis carried out here in an industrial case shows the importance of the coupling mode phenomenon when structure hydro-elastic modes and fluid acoustic modes are of the same order. De Langre [28] introduced the following non-dimensional number in order to evaluate the coupling effect:

$$\mathrm{A} = \frac{c}{\sqrt{E / \rho_S}} \tag{50}$$

A is the ratio between the celerity of acoustic waves in the fluid media and the elastic waves in the structure media. When A is close to unity, elasto-acoustic mode coupling is

observed. This approach remains limited to a global description of the coupling process and is valid for the first coupled eigenmode.

Elastic energy of the coupled fluid-structure system can be calculated as:

$$\varepsilon_{ela(\mathbf{u},p,\varphi)} = \frac{1}{2}\int_{\Omega} \rho_F c^2 \left(\nabla\varphi\right)^2 d\Omega_F + \frac{1}{2}\int_{\Sigma_k} \sigma_{ij}(\mathbf{u}_k)\varepsilon_{ij}(\mathbf{u}_k) d\Sigma_k \tag{51}$$

where **u** is the structure displacement and φ is the fluid potential displacement. The potential energy is the sum of the fluid elastic energy and the structure elastic energy, this latter being calculated as:

$$\varepsilon^s_{ela(\mathbf{u})} = \frac{1}{2}\int_{\Sigma_k} \sigma_{ij}(\mathbf{u}_k)\varepsilon_{ij}(\mathbf{u}_k) d\Sigma_k \tag{52}$$

Denoting $\mathbf{K}$ and $\mathbf{K}_S$ the stiffness matrix for the coupled and structure problem, and $\mathbf{X}_n = \left\langle \mathbf{U}_n, \mathbf{P}_n, \mathbf{\Phi}_n \right\rangle$ the coupled eigenmodes, the potential energy of each mode is the calculated as:

$$\varepsilon_{ela(\mathbf{u},p,\varphi)} = \frac{1}{2}\mathbf{X}_n^T \mathbf{K} \mathbf{X}_n \tag{53}$$

and the elastic structure energy part in the total energy is given by:

$$\varepsilon^s_{ela(\mathbf{u})} = \frac{1}{2}\mathbf{U}_n^T \mathbf{K}_S \mathbf{U}_n \tag{54}$$

The elasto-acoustic coupling can then be evaluated for each mode by calculating the following ratio:

$$\Lambda = \frac{\varepsilon_{ela(\mathbf{u},p,\varphi)} - \varepsilon^s_{ela(\mathbf{u})}}{\varepsilon_{ela}(\mathbf{u},p,\varphi)} \tag{55}$$

Λ is the ratio between the amount of "fluid elastic energy" over the "total elastic energy" in the system. From the practical point of view, is calculated with the following relation:

$$\Lambda = 1 - \frac{\mathbf{U}_n^T \mathbf{K}_S \mathbf{U}_n}{\mathbf{X}_n^T \mathbf{K} \mathbf{X}_n} \tag{56}$$

Table 3 Λ ratio for the first six fluid-structure eigenmodes

Mode	Hydro-elastic case	Elasto-acoustic case
#1	0.0%	3.0%
#2	0.0%	4.4%
#3	0.0%	36.0%
#4	0.0%	37.0%
#5	0.0%	47.0%
#6	0.0%	37.0%

For a pure structure system, it is null by definition; for a structure coupled with an incompressible fluid, Λ is also null. For any elasto-acoustic coupled system (elastic structure coupled with acoustic fluid), $0 \leq \Lambda \leq 1$; the greater Λ is, the more important elasto-acoustic coupling is.

Table 3 gives the computed values of Λ for the first six eigenmodes, in the hydro-elastic case (elastic structure coupled with incompressible fluid) and the elasto-acoustic case.

As expected in the hydro-elastic case, $\Lambda \equiv 0$ for all eigenmodes. In the elasto-acoustic case at operating conditions, Λ is a few percent for the first two modes, for which fluid compressibility has limited influence, as pointed out before. Λ reaches much higher values (around 40%) from the third mode, which has been identified as the first coupled elasto-acoustic eigenmode. All following modes are more or less affected by coupling phenomenon (i.e. by fluid compressibility) and are thus characterized by high values of Λ.

The proposed ratio Λ thus gives a good evaluation of the coupling effect in an elasto-acoustic system, mode per mode, instead of the global indication given by the ratio A, which however remains a pertinent tool for a priori analyse.

3.2.5. Structure coupled with fluid, with internal structure modelling

When taking into account the internal structures through the homogenised fluid, coupling effects are modified as follows. Eigenmode shapes are quite similar with those calculated with the incompressible fluid model. However, influence of confinement on eigenfrequencies is more significant: the first coupled mode is a flexion mode of the inner structure, at frequency 21.3 Hz. The influence of inner inclusions on this mode is significant in term of added mass (the frequency of the mode is decreased from –13%) since the solid inclusions tend to limit the fluid motions and thus increase the added mass. The second mode is a fluid-coupled inner-outer structure mode, at frequency 64.8 Hz. Influence of fluid confinement on that mode is also significant since the shift in frequency is about –15%. Influence on the third mode (at frequency 82.7 Hz) is as significant as for the second mode.

It can be inferred from the modal analysis that the predominant fluid-structure interaction effects in the case of the nuclear reactor studied here are:

– Inertia coupling in the low frequency range (under 100 Hz);
– Elasto-acoustic coupling effects in the high frequency range (above 100 Hz).

In both cases, FSI effects are increased as a result of confinement induced by the presence of internal structures. In dynamic (seismic and shock) analysis presented in the next subsection, fluid-structure interaction will hence be modelled using the homogenisation approach with fluid compressibility.

4. DYNAMIC ANALYSIS OF THE NUCLEAR REACTOR WITH FLUID-STRUCTURE INTERACTION

4.1. ANALYSIS PRINCIPLE

The problem of interest in the present paper is to compute the response of a linear system subjected to an imposed acceleration, such as a seism or a shock. The dynamic load on the system is described by the acceleration profile $\gamma(t)$ in a given direction $\mathbf{D}$ and the system response is defined by the evolution of its degrees of freedom $\mathbf{X}(t)$ (e.g. in the context of fluid-structure interaction problems, structure displacement field and fluid pressure and displacement potential fields) in the moving frame. $\mathbf{M}$, $\mathbf{C}$ and $\mathbf{K}$ denoting respectively the system mass, damping and stiffness matrices, the system dynamic is described by the following equation [29,30]:

$$\mathbf{M}\ddot{\mathbf{X}}(t) + \mathbf{C}\dot{\mathbf{X}}(t) + \mathbf{K}\mathbf{X}(t) = -\mathbf{M}\mathbf{D}\gamma(t) \tag{57}$$

The computation of the dynamic response of the nuclear reactor can be performed with various approaches.

4.1.1. Direct time integration method

Computation of the system response can be performed with direct time integration methods, i.e. solving Eq. (57) with finite difference schemes, either with explicit [31] or implicit [32] approaches.

Substituting approximation of the system acceleration $\ddot{\mathbf{X}}_{k+1} = \ddot{\mathbf{X}}(t_{k+1})$ and velocity $\dot{\mathbf{X}}_{k+1} = \dot{\mathbf{X}}(t_{k+1})$ at time step t_{k+1} and using the system acceleration $\ddot{\mathbf{X}}_k = \ddot{\mathbf{X}}(t_k)$, velocity $\dot{\mathbf{X}}_{k+1} = \dot{\mathbf{X}}(t_{k+1})$ and displacement $\mathbf{X}_k = \mathbf{X}(t_k)$ yields for instance the Newmark scheme (Newmark, 1954):

$$\begin{aligned}(\frac{\mathbf{M}}{\beta\delta t^2} + \frac{\mathbf{C}}{\beta\delta t} + \mathbf{K})\mathbf{X}_{k+1} &= -\mathbf{M}\mathbf{D}\gamma_{k+1} + (\frac{\mathbf{M}}{\beta\delta t^2} + \frac{\mathbf{C}}{\beta\delta t})\mathbf{X}_k \\ +(\frac{\mathbf{M}}{\beta\delta t} - \mathbf{C}(1 - \frac{\alpha}{\beta}))\dot{\mathbf{X}}_k &+ (\mathbf{M} + \mathbf{C}\alpha\delta t)(\frac{1}{2\beta} - 1)\ddot{\mathbf{X}}_k\end{aligned} \tag{58}$$

All terms in the right hand side of Eq. (58) are known quantities; computation of X_{k+1} is straightforward and requires the inversion of the matrix $\tilde{\mathbf{K}} = \frac{\mathbf{M}}{\beta\delta t^2} + \frac{\mathbf{C}}{\beta\delta t} + \mathbf{K}$. For linear problems, **M**, **C** and **K** are time independent, thus inversion of $\tilde{\mathbf{K}}$ has just to be performed once at the first time step of the algorithm.

4.1.2. Modal time integration method

Direct integration methods are rather time consuming, even with nowadays computers and with rather simple finite element models. It is then more efficient to use a projection of Eq. (1) onto a suitable vector basis in order to solve a set of ordinary differential equations [33]. Projection is made possible by expanding the problem unknown **X**(**x**,t) as:

$$\mathbf{X}(\mathbf{x}, t) = \sum_{n>0} \xi_n(t)\mathbf{X}_n(\mathbf{x}) \tag{59}$$

where $(\mathbf{X}_n)_{n>0}$ is a vector basis and $(\xi_n)_{n>0}$ are the generalised coordinates of vector **X**. The major interest of decomposition (60) is clearly to separate the time and space dependency of the system degrees of freedom into the coordinates $\xi_n(t)$ on the one hand, and the basis vector $\mathbf{X}_n(x)$ on the other hand.

The most appropriate vector basis is that of the system eigenvectors, those latter being the solutions of the eigenvalue problem:

$$(-\omega_n^2\mathbf{M} + \mathbf{K})\mathbf{X}_n = \mathbf{0} \tag{60}$$

with ω_n the eigenpulsation associated with eigenvector $\mathbf{X}_n$.

When **M** and **K** are symmetric and positive definite matrices, the eigenvectors form a basis of the problem and comply with the following orthogonality conditions:

$$\mathbf{X}_n^T \mathbf{M} \mathbf{X}_{n'} = \delta_{n,n'} m_n \qquad \mathbf{X}_n^T \mathbf{K} \mathbf{X}_{n'} = \delta_{n,n'} k_n \tag{61}$$

where $\delta_{n,n'}$ stands for the Kronecker symbol. m_n and k_n are referred to as the modal mass and modal stiffness of eigenvector $\mathbf{X}_n$, respectively. The system dynamic behaviour can then be viewed as the superposition of elementary mass-spring systems with mass m_n and spring stiffness k_n, each system oscillating at frequency f_n, given by:

$$f_n = \frac{1}{2\pi} \sqrt{\frac{k_n}{m_n}} \tag{62}$$

Substituting the modal decomposition (60) into Eq. (57), multiplying each term by $\mathbf{X}_n^T$ and using the orthogonality conditions given by Eq. (62), yields the following set of equations:

$$\ddot{\xi}_n(t) + \frac{(\mathbf{X}_n^T \mathbf{C} \mathbf{X}_n)}{m_n} \dot{\xi}_n(t) + \omega_n^2 \xi_n(t) = -\kappa_n \gamma(t) \tag{63}$$

where κ_n is the participation factor of eigenmode $\mathbf{X}_n$, defined as:

$$\kappa_n = \frac{\mathbf{X}_n^T \mathbf{M} \mathbf{D}}{\mathbf{X}_n^T \mathbf{M} \mathbf{X}_n} \tag{64}$$

The participation factor can be interpreted as a shape factor which indicates how eigenmode $\mathbf{X}_n$ is to respond to the imposed acceleration in direction $\mathbf{D}$: the higher κ_n is, the greater the effect of shock on eigenmode $\mathbf{X}_n$ is. As a limit case, when $\mathbf{X}_n$ and $\mathbf{D}$ are orthogonal with respect to the mass weighted scalar product $\mathbf{X}_n^T \mathbf{M} \mathbf{D}$, then $\kappa_n = 0$, indicating that eigenmode $\mathbf{X}_n$ contribution on the system response is null. In order to obtain a set of decoupled equations, it is convenient to use the proportional damping model, i.e. assuming that the damping matrix can be written:

$$\mathbf{C} = \lambda \mathbf{M} + \mu \mathbf{K} \tag{65}$$

where λ and μ are the Raleigh coefficients. Illustration and physical interpretation of the proportional damping model, with simple yet powerful elementary models from the engineering point of view, can be found for instance in [4].

Substituting Eq. (65) into Eq. (63) finally yields the following set of equations:

$$\ddot{\xi}_n(t) + 2\beta_n \omega_n \dot{\xi}_n(t) + \omega_n^2 \xi_n(t) = -\kappa_n \gamma(t) \tag{66}$$

where β_n is the modal damping of eigenmode $\mathbf{X}_n$. According to Eq. (11) and to the orthogonality conditions given by Eq. (62), βn is deduced from the Raleigh coefficient as:

$$\beta_n = \frac{\lambda}{2\omega_n} + \frac{\mu \omega_n}{2} \tag{67}$$

Setting β for two particular modes XI and XII, of eigenpulsation ωI and ωII respectively, defines the value of λ and μ.

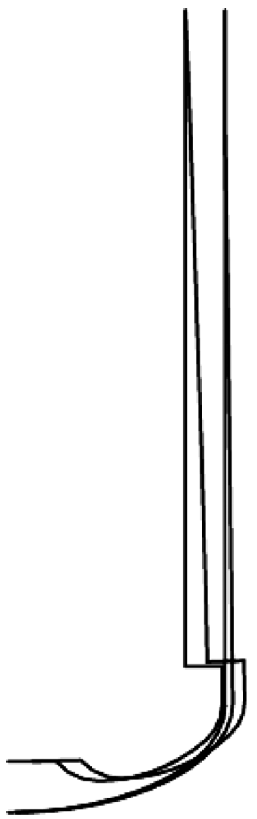

Figure 9 Seismic analysis with static approach: deformation of the structure.

Time integration of each modal equation of as Eq. (66) can be performed with numerical methods for ordinary differential equations. In practice, few eigenmodes have to be retained in the analysis to give an accurate description of the system behaviour. Computational time can then drastically reduced by using time integration with modal decomposition techniques.

4.1.3. Spectral method

Computation of a mechanical system response with direct or modal time integration techniques is possible when the imposed loading is defined by an accelerogram $t \mapsto \gamma(t)$, which defines the imposed acceleration for each time step. From the engineering point of view, shock or seism loading are often characterised by a response spectrum. It is recalled that the response spectrum plots for each possible value of ω the maximum displacement ξ(ω,β,γ) of a single degree of freedom system, defined by its pulsation ω and damping coefficient β and subjected to the acceleration γ [30]. By definition, ξ(ω,β,γ) = maxt > 0 ξ(t), where ξ(t) is the solution of ξ(t) + 2βωξ(t) + ω2ξ(t) = –γ(t). Representation of a dynamic loading through its response spectrum enables a simple comparison of various imposed loads [34]. Response spectrum are usually represented in terms of static equivalent (or pseudo) acceleration, i.e. by plotting $\omega \mapsto \Gamma(\omega,\beta,\gamma)$ where $\Gamma(\omega,\beta,\gamma) = \omega^2 \times \delta(\omega,\beta,\gamma)$. Example of shock response spectrum is given in subsection 4. By construction, a response spectrum only gives indication on the maximum value of displacement or acceleration of a single

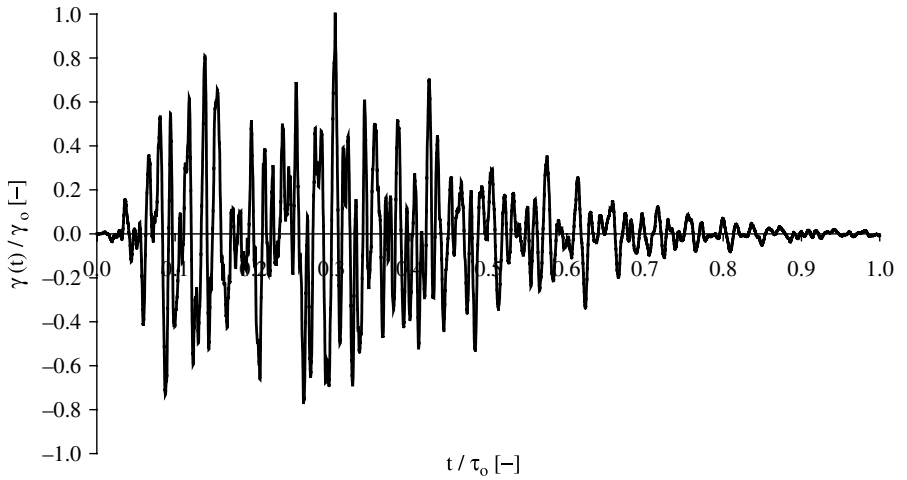

Figure 10 Shock signal: non dimensional accelerogram t/τ_o?$\gamma(t)/\gamma_o$.

degree of freedom system; an estimation of the maximum displacement or acceleration of a linear system can be obtained with spectral approach. Since each eigenmode contribution on the system response is described by the equation of motion of a single degree of freedom system, it can be deduced from the response spectrum the maximum value of each modal coordinate $\xi_n(t)$ according to:

$$\max_{t\geq 0}\left|\xi_n(t)\right| = \left|\kappa_n\right| \times \frac{\Gamma(\omega_n, \beta_n, \gamma)}{\omega_n^2} \tag{69}$$

Thus, the maximum value of the system displacement $\left\|\mathbf{X}(\mathbf{x},t)\right\|$ at a given location x can then be estimated from a combination of each eigenmode contribution $\left|\kappa_n\right| \times \frac{\Gamma(\omega_n, \beta_n, \gamma)}{\omega_n^2}\left\|\mathbf{X}_n(\mathbf{x})\right\|$, for all n. For instance, a quadratic combination yields:

$$\max_{t\geq 0}\left\|\mathbf{X}(\mathbf{x},t)\right\| \equiv \sqrt{\sum_n \left(\left|\kappa_n\right| \times \frac{\Gamma(\omega_n, \beta_n, \gamma)}{\omega_n^2}\left\|\mathbf{X}_n(\mathbf{x})\right\| \right)^2} \tag{70}$$

The number of eigenmode to retain in the spectral analysis has to be sufficient enough to accurately describe the system response. A criterion which is commonly applied in seismic analysis of structures [29], is based on the evaluation of the effective mass μ_n. It is recalled that the effective mass of eigenmode $\mathbf{X}_n$ is defined as:

$$\mu_n = \frac{\left(\mathbf{X}_n^T \mathbf{M} \mathbf{D}\right)^2}{\mathbf{X}_n^T \mathbf{M} \mathbf{X}_n} \tag{71}$$

and that summation of effective masses gives the system mass, in other words $\sum_n \mu_n = m$. Therefore, in spectral methods, it is necessary to use a modal basis with $\sum_n \mu_n$ as close to m as possible, in order to have a good estimation of the system dynamic response.

4.1.3. Static method

When the typical loading frequency is lower than the lowest system eigenfrequency, the system behaves in a quasi-static manner. "Dynamic" response of the system can in this case be safely described by neglecting inertial effects, i.e. using a static acceleration representation of the seismic signal. In such a case, Eq. (57) reduces to:

$$\mathbf{KX} = -\mathbf{MD}\gamma_o \tag{72}$$

where γ_o is the value of the static equivalent acceleration. The static method thus requires the resolution of a linear system which can be performed either with direct or modal methods.

4.2. INDUSTRIAL APPLICATION

4.2.1. Seismic analysis

The typical frequency of the seismic loading is about 25–30 Hz. As highlighted by the modal analysis with fluid-structure modelling, the first eigenfrequency of the predominant mode (i.e. mode with the highest effective mass) system is 64.8 Hz so that the reactor behaviour under seismic loading is quasi-static. Seismic analysis can be performed with a static approach. In order to highlight the influence of fluid, static analysis of the system with and without fluid-structure coupling is carried out. The maximum computed displacement of the inner and outer structures are summarised in Table 4. Calculations are performed with a static acceleration of amplitude 1 m/s^2 in the transverse direction. Deformations of the inner and outer structures under static acceleration are represented by Fig. 9.

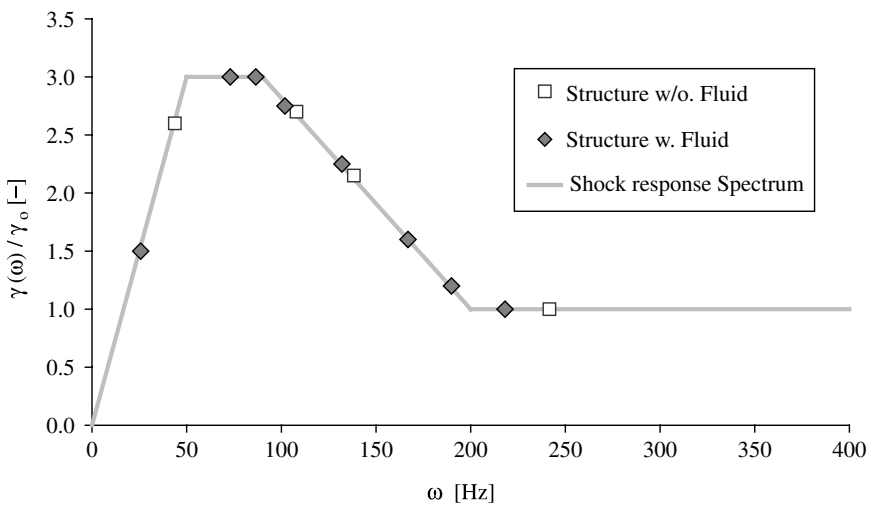

Figure 11 Shock response spectrum and coupled eigenmodes.

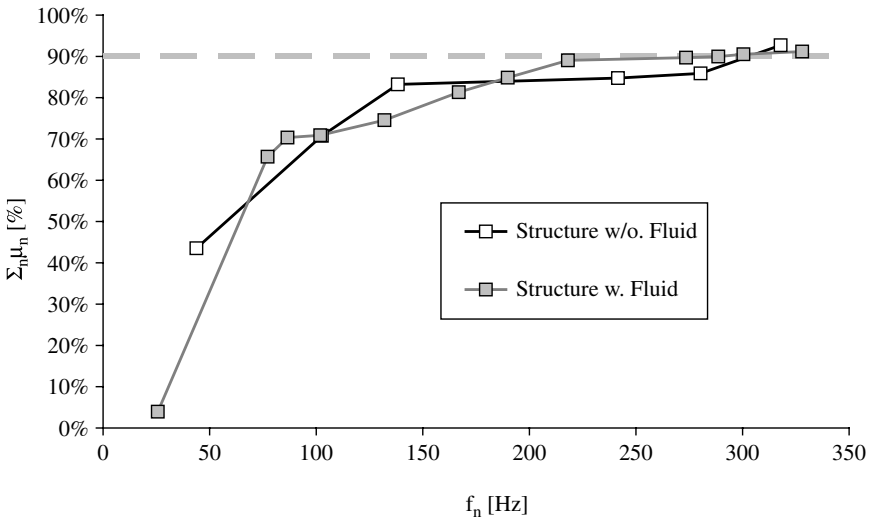

Figure 12 Cumulated effective masses versus frequencies of the nuclear reactor with and without fluid-structure interaction.

Table 4 Seismic and shock analysis of the nuclear reactor with and without fluid structure interaction

Maximum displacement of structure	**Without fluid**	**With fluid**
Seismic analysis, static calculation		
Inner structure	$1.77*10^{-5}$ m	$1.20*10^{-5}$ m
Outer structure	$0.26*10^{-5}$ m	$0.39*10^{-5}$ m
Shock analysis, temporal calculation		
Inner structure	$4.58*10^{-5}$ m	$1.46*10^{-5}$ m
Outer structure	$0.60*10^{-5}$ m	$1.40*10^{-5}$ m
Shock analysis, spectral calculation		
Inner structure	$4.57*10^{-5}$ m	$1.44*10^{-5}$ m
Outer structure	$0.62*10^{-5}$ m	$1.39*10^{-5}$ m

The calculated displacement for the inner structure with fluid is less than without fluid, whereas the opposite observation can be drawn for the outer structure. This results from static fluid force acting against the imposed acceleration on the inner structure, and together with the imposed acceleration on the outer structure [9].

4.2.2. Shock analysis

A typical accelerogram of shock imposed on the system is given in Fig. 10 in non-dimensional coordinate system, with γ_o standing for the maximum acceleration and τ_o for shock duration.

Figure 11 gives the corresponding Shock Response Spectrum. Frequencies of the reactor with and without fluid have been identified in the SRS: dynamic behaviour of the system is clearly governed by several eigenmodes. As a consequence static approach is not relevant for shock analysis. Temporal method with modal approach or spectral method are then preferred.

As mentioned in the preceding subsection, it is then necessary to take enough modes into account. In the present study, the number of modes to retain in the analysis is such that 90% of the total system mass is accounted for. Figure 12 plots the cumulated effective masses versus frequency: in order to take 90% of the total mass, six modes are needed for the structure alone and twelve modes for the structure coupled with fluid.

According to engineering recommendations and common practice for such analysis, damping coefficients have been set to 5% for the two predominant eigenmodes (in terms of effective mass). Damping coefficients for other eigenmodes are deduced using Eq. (67).

Under these assumptions, shock analysis can be performed. Table 5 gives the maximum calculated displacement of the inner and outer structure, using temporal or spectral methods, with and without fluid-structure coupling.

Identical trends as in the seismic analysis can be highlighted: the inner structure displacement is lower when fluid-structure interaction is accounted for, while the opposite stands for the outer structure. From the engineering standpoint, this illustrated the importance of FSI in the dynamic response of the nuclear reactor when subjected to shock. In design stages, a complete three-dimensional analysis of the reactor with fluid structure interaction modelling will then be required.

In addition, it should be noticed that the temporal and spectral approaches give identical results in terms of displacement calculation. This validates the use of such methods for future design studies of propulsion nuclear reactors, as long as FSI is accounted for. Since all industrial finite element codes do not allow spectral calculation with fluid-structure interaction, specific developments are therefore carried out in DCNS finite element code for future industrial applications [11,35].

5. CONCLUSION

A global analysis of fluid-structure interaction effects has been carried out for a simplified model of a nuclear reactor, using various numerical models and various engineering approaches. Dynamic analysis has also been performed in order to study the reactor behaviour under seismic and shock loading, using a numerical method which is consistent with the physics of the system. Several conclusions can be drawn from the presented analysis, from methodological, numerical and industrial standpoints.

- From the methodological point of view, various modelling of fluid-structure effects have been investigated (static loading, inertial coupling, elasto-acoustic coupling, and confinement effects) and application of the coupled analysis in the context of systems subjected to dynamic loading has been considered. Modal techniques (for temporal and spectral methods) have also been applied in the context of seismic and shock analysis of structures with fluid-structure interaction modelling.
- From the numerical point of view, a homogenisation approach has been developed for the modelling of the reactor internal structures with fluid-structure interaction. The proposed method allows a rather straightforward modelling of internal structures without requiring a complete mesh of the structures geometry. The method enables the use of a 2D axi-symmetric model and produces a correct calculation of the eigenmodes, eigenfrequencies and effective masses, which is of paramount importance for shock or seismic analysis purposes.

– From the industrial point of view, inertial coupling have been proved of paramount importance (for seismic analysis), while elasto-acoustic coupling effects have significant influence on the dynamic behaviour of the reactor in the high frequency range (for shock analysis). In both cases, confinement induced by the presence of the internal reactor structures has also been analysed and has noticeable effect on increasing inertial effects. On the other hand, coupled calculation with inner pressure correction terms indicates that the pre-stress effect has little influence on the dynamic behaviour of the reactor. It is then demonstrated that static (pressure resistance) and dynamic (modal analysis with fluid-structure interaction) design can be performed separately, as it is indeed current practice in design office.

Additional developments of fluid-structure interaction modelling in naval nuclear propulsion systems are currently under investigation. In particular, application of the homogenisation method presented in the paper to the numerical study of tube bundle in steam generator is studied.

ACKNOWLEDGMENT

The author wishes to thank M.M. GUILLOPÉ and GALVICIC from STXN for continuously supporting the scientific exchanges between CEA and DCNS with R&D programs on fluid-structure interaction modelling.

NOMENCLATURE

ω,ω_n = pulsation, eigenpulsation
ξ_n = modal coordinate
β_n = modal damping
μ_n = modal effective mass
κ_n = modal participation factor
$\varepsilon^s_{ela},\varepsilon^f_{ela},\varepsilon_{ela}$ = structure, fluid and fluid-structure elastic energy
$\varepsilon^s_{kin},\varepsilon^f_{kin},\varepsilon_{kin}$ = structure, fluid and fluid-structure kinetic energy
γ = imposed acceleration (shock or seism)
$\Gamma(\omega_n,\beta_n,\gamma)$ = pseudo acceleration at eigenpulsation ω_n and damping β_n for acceleration γ
$\mathbf{D}$ = direction of imposed acceleration
$\mathbf{K}_S$, $\mathbf{K}_F$ = structure/fluid stiffness matrices
$\mathbf{K}_\pi$, $\mathbf{K}_\sigma$ = structure added stiffness matrices
$\mathbf{K}$ = stiffness matrix
$\mathbf{M}_S$, $\mathbf{M}_F$ = structure/fluid mass matrices
$\mathbf{M}$ = stiffness matrix
$\mathbf{R}_k$ = fluid-structure interaction matrix
$\mathbf{H}$ = fluid-structure coupling matrix
ρ_S, ρ_F = structure/fluid density
c = acoustic wave velocity
$\mathbf{U}_k$ = structure displacement degrees of freedom
$\mathbf{P}$ = fluid pressure degrees of freedom
Φ = fluid displacement potential degrees of freedom
$\mathbf{X}_n$ = eigenmode

Σ_k = structure domain
Ω = fluid domain
Ω^* = homogenised fluid domain
Γ_k = fluid-structure interface
Ω_S = solid inclusion domain
Ω_F = fluid elementary domain
Ω_T = elementary cell domain
I, J = confinement ratios
$\mathbf{u}_k$ = structure displacement field
$\varepsilon(\mathbf{u}_k)$ = structure strain tensor
$\sigma(\mathbf{u}_k)$ = structure stress tensor
$\mathbf{U}_F$, $\ddot{\mathbf{U}}_F$ = global fluid displacement/acceleration
$\mathbf{u}_F$, $\ddot{\mathbf{u}}_F$ = local fluid displacement/acceleration
$\mathbf{u}_S$, $\ddot{\mathbf{u}}_S$ = internal structure displacement/acceleration
ψ_o = axi-symmetric Fourier mode
ψ_s = symmetric Fourier mode
ψ_a = anti-symmetric Fourier mode

REFERENCES

[1] J. Makerle. Fluid-structure interaction problems, finite element approach and boundary elements approaches. A Bibliography. *Finite Elements in Analysis and Design,* 31, 231–240, 1999.

[2] J. Makerle. Earthquake analysis of structures: FEM and BEM approaches, a bibliography (1995–1998). *Finite Element Analysis Design,* 32, 113–124, 1999.

[3] J. Makerle. Finite element vibration and dynamic response analysis of engineering structures, a bibliography (1994–1998). *Shock and Vibration,* 7, 39–56, 2000.

[4] F. Axisa. *Modelling of mechanical systems. Vol 3. Fluid-structure interaction.* Elsevier, 2006.

[5] R.J. Gibert. *Vibration des structures. Interactions avec les fluides. Sources d'excitation aléatoires.* Collection de la Direction des Etudes et Recherches d'Electricité de France, vol. 69, Eyrolles, 1986.

[6] H. J.-P. Morand, R. Ohayon. *Fluid-structure interaction.* Wiley & Sons, 1995.

[7] J.F. Sigrist, D. Broc, C. Lainé. Dynamic analysis of a nuclear reactor with fluid-structure interaction. Part I: seismic loading, fluid added mass and added stiffness effects. *Nuclear Engineering and Design,* 236, 2431–2443, 2006.

[8] J.F. Sigrist, D. Broc, C. Lainé. Dynamic analysis of a nuclear reactor with fluid-structure interaction. Part II: shock loading, fluid compressibility effects. *Nuclear Engineering and Design,* 237, 289–299, 2007.

[9] R.J. Fritz. The effect of liquids on the dynamic motion of immersed solids. *Journal of Engineering for Industry,* 94, 167–173, 1972.

[10] C. Rajakumar, C. G. Rogers. The Lanczos algorithm applied to unsymmetric generalized eigenvalue problem. *International Journal of Numerical Methods in Engineering,* 32, 1009–1026, 1991.

[11] J.F. Sigrist. Modal analysis of fluid-structure interaction problems with pressure-based finite elements for industrial applications. *International Journal of Multiphysics,* 1, 123–149, 2007.

[12] G.C. Everstine. A symmetric potential formulation for fluid-structure interaction. *Journal of Sound and Vibration,* 79, 157–190, 1981.

[13] G. Sandberg, P.A., Göransson. A symmetric finite element formulation for acoustic fluid-structure interaction analysis. *Journal of Sound and Vibration,* 123, 507–515, 1988.

[14] F. Axisa, R.J. Gibert. *Non-linear analysis of fluid-structure coupled transient problems in piping systems using finite elements. Application to the mechanical effects in sodium-water reaction in the secondary loop of a pool-type LMFBR*. Pressure Vessel and Piping, Orlando, 27 June–2 July, 1982.

[15] H. J-P. Morand, R. Ohayon. Substructure variationnal analysis of the vibrations of coupled fluid-structure systems. Finite element results. *International Journal for Numerical Methods in Engineering,* 14, 741–755, 1979.

[16] J.F. Sigrist, D. Broc. Homogenisation method for the modal analysis of a nuclear reactor with internal structures modelling and fluid structure-interaction coupling. *Nuclear Engineering and Design,* 237, 431–440, 2007.

[17] A. Bensoussan, J.L. Lions, G. Papanicolaou. *Asymptotic analysis for periodic structures*. North-Holland, 1978.

[18] E. Sanchez-Palencia. *Non-homogenous media and vibration theory.* Springer-Verlag, 1980.

[19] C. Conca, J. Planchard, M. Vanninathan. *Fluids and periodic structures*. Masson, 1995.

[20] J. Planchard. Eigenfrequencies of a tube bundle placed in a confined fluid. *Computer Methods in Applied Mechanics and Engineering,* 30, 75–93, 1982.

[21] J. Planchard, M. Ibnou-Zahir. Natural frequencies of a tube bundle in an incompressible fluid. *Computer Methods in Applied Mechanics and Engineering,* 41, 47–68, 1983.

[22] L. Hammami. *Etude de l'interaction fluide/structure dans les faisceaux de tubes par une méthode d'homogénéisation. Application à l'analyse sismique des cœurs RNR*. Thèse de Doctorat, Univeristé Paris VI, 1991.

[23] D. Brochard, F. Gatenbein, R.J. Gibert. *Modelling of the dynamic behaviour of LWR internals. 9th Conference on Structural Mechanic in Reactor Technology,* Lausane, 17–21 August, 1987.

[24] K. Cheval. *Modélisation du comportement sismique de structures multitubulaires baignées par un fluide dense*. Thèse de Doctorat, Université Paris VI, 2001.

[25] D. Broc, J.C. Queval, E. Viallet. *Seismic behaviour of PWR reactor cores: fluid-structure effects.* 17th Conference on Structural Mechanic in Reactor Technology, Prague, 17–22 August, 2003.

[26] D. Broc. *Seismic behaviour of PWR reactor cores: whole core model with fluid-structure interaction effects*. Flow Induced Vibrations, Paris, 6–9 July, 2004.

[27] P. Verpeaux, A. Millard, T. Charras, A. Combescure. *A modern approach of computer codes for structural analysis*. Structural Mechanics in Reactor Technology, Anaheim, 14–18 August, 1989.

[28] E. De Langre. *Fluides et solides*. Les éditions de l'Ecole Polytechnique, 2001.

[29] R.W. Clough, J. *Penzein. Dynamics of structures*. MacGraw-Hill, 1986.

[30] C.M. Harris. *Shock and vibration handbook*. MacGraw-Hill, 1998.

[31] M.A. Dokainish, K. Subbaraj. A Survey of direct time-integration methods in computational structural dynamics-I. Explicit methods. *Computer & Structures,* 32, 1371–1386, 1989.

[32] K. Subbaraj, M.A. Dokainish. A Survey of direct time-integration methods in computational structural dynamics-II. Implicit methods. *Computer & Structures,* 32, 1387–1401, 1989.

[33] K.J. Bathe. *Finite element procedures in engineering analysis*. Prentice-Hall, 1982.

[34] A.K. Gupta, T. Hassan. *Time and frequency domain analysis of single degrees of freedom systems*. Nuclear Engineering and Design, 167, 1–5, 1996.

[35] J.F. Sigrist, S. Garreau. Dynamic analysis of fluid-structure interaction problems with spectral method using pressure-based finite elements. *Finite Element Analysis in Design,* 43, 287–300, 2007.